

# Substituted 2-Aminopyrimidines Selective for $\alpha 7$ -Nicotinic Acetylcholine Receptor Activation and Association with Acetylcholine Binding Proteins

Katarzyna Kaczanowska,<sup>†,‡</sup> Gisela Andrea Camacho Hernandez,<sup>‡,†,||</sup> Larissa Bendiks,<sup>†</sup> Larissa Kohs,<sup>†</sup> Jose Manuel Cornejo-Bravo,<sup>||</sup> Michal Harel,<sup>†,§</sup> M. G. Finn,<sup>⊥</sup> and Palmer Taylor<sup>\*,†,||</sup>

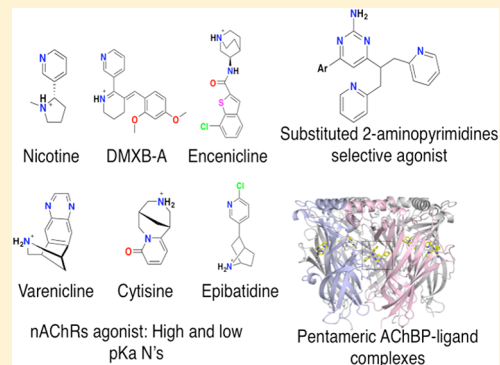
<sup>†</sup>Department of Pharmacology, Skaggs School of Pharmacy & Pharmaceutical Sciences, University of California, San Diego, La Jolla, California 92093-0650, United States,

<sup>||</sup>Facultad de Ciencias Químicas e Ingeniería, Universidad Autónoma de Baja California, Calzada Universidad 14418, Tijuana, Baja California 22390, Mexico

<sup>⊥</sup>School of Chemistry and Biochemistry, Georgia Institute of Technology, Atlanta, Georgia 30332, United States

## Supporting Information

**ABSTRACT:** Through studies with ligand binding to the acetylcholine binding protein (AChBP), we previously identified a series of 4,6-substituted 2-aminopyrimidines that associate with this soluble surrogate of the nicotinic acetylcholine receptor (nAChR) in a cooperative fashion, not seen for classical nicotinic agonists and antagonists. To examine receptor interactions of this structural family on ligand-gated ion channels, we employed HEK cells transfected with cDNAs encoding three requisite receptor subtypes:  $\alpha 7$ -nAChR,  $\alpha 4\beta 2$ -nAChR, and a serotonin receptor (5-HT<sub>3A</sub>R), along with a fluorescent reporter. Initial screening of a series of over 50 newly characterized 2-aminopyrimidines with affinity for AChBP showed only two to be agonists on the  $\alpha 7$ -nAChR below 10  $\mu$ M concentration. Their unique structural features were incorporated into design of a second subset of 2-aminopyrimidines yielding several congeners that elicited  $\alpha 7$  activation with EC<sub>50</sub> values of 70 nM and K<sub>d</sub> values for AChBP in a similar range. Several compounds within this series exhibit specificity for the  $\alpha 7$ -nAChR, showing no activation or antagonism of  $\alpha 4\beta 2$ -nAChR or 5-HT<sub>3A</sub>R at concentrations up to 10  $\mu$ M, while others were weaker antagonists (or partial agonists) on these receptors. Analysis following cocrystallization of four ligand complexes with AChBP show binding at the subunit interface, but with an orientation or binding pose that differs from classical nicotinic agonists and antagonists and from the previously analyzed set of 2-aminopyrimidines that displayed distinct cooperative interactions with AChBP. Orientations of aromatic side chains of these complexes are distinctive, suggesting new modes of binding at the agonist-antagonist site and perhaps an allosteric action for heteromeric nAChRs.



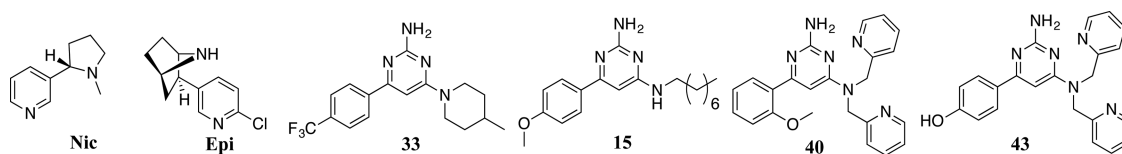
## INTRODUCTION

Up to 12 different subunits ( $\alpha 2$ –10 and  $\beta 2$ –4) assemble with selectivity into closely related pentameric subtypes of nicotinic acetylcholine receptors (nAChRs) found in mammalian brain.<sup>1–5</sup> These receptors are widely distributed throughout the central and peripheral nervous systems and elicit a variety of physiological responses. The nAChRs consist of homo- and heteropentameric structures and belong to the Cys-loop superfamily of ligand-gated ion channels. The diverse assemblies of subunits, together with their discrete regional tissue locations, define the functional activity and the pharmacological responses of these receptors. Structurally, a large N-terminal extracellular domain, followed by four transmembrane spans with intervening intracellular domains, is found in each subunit that assembles to form the functional pentameric nAChR.

The primary orthosteric ligand binding pocket for agonists and competitive antagonists is localized in the extracellular domain at the interface between the principal ( $\alpha$ ) and a complementary subunit. These sites are only identical for the homomeric  $\alpha 7$ -nAChRs. Several candidate locations for allosteric binding sites have also been identified on nAChR subtypes.<sup>4,6,7</sup> Soluble acetylcholine binding proteins (AChBPs) from mollusks are known to have a spectrum of ligand binding affinities, similar to the homopentameric  $\alpha 7$ -nAChR. Critical amino acid residues identified in the nAChR ligand-binding domain are largely identical or homologous in AChBP.<sup>8</sup> Recent analyses of the crystal structures<sup>9–13</sup> along with other physical and ligand binding properties of AChBPs<sup>14,15</sup> from *Lymnaea*

Received: October 28, 2016

Published: February 21, 2017

Chart 1. Nicotine (Nic), Epibatidine (Epi), Cooperative AChBP Ligands (33, 15), and Novel Agonists (40, 43) of the  $\alpha 7$ -nAChR

*stagnalis* (*Ls*) and *Aplysia californica* (*Ac*) have assisted in defining molecular recognition for ligands.

With a series of 4,6-substituted 2-aminopyrimidines and AChBP, we have conducted crystallographic studies that show that this family of ligands bind at the classical agonist–antagonist site, displace epibatidine, but in so doing, exhibit unusual cooperative binding and conformational state changes in the pentameric AChBP.<sup>16</sup> This family of approximately 50 congeneric 4,6-substituted 2-aminopyrimidines show a range of binding affinities and three classes of cooperativity profiles toward *Ls*-AChBP as classic nicotine-like ( $n_H = 1$ ), positively cooperative ligands ( $n_H > 1$ ) with moderate binding affinity, and exceptionally potent negatively cooperative ligands ( $n_H < 1$ ). While all three groups exhibited binding selectivity toward *Ls*-AChBP and lead crystal structures could be determined,<sup>16</sup> all but two failed to activate or block  $\alpha 7$  nAChRs at concentrations below 10  $\mu$ M. Herein, we synthesize and characterize a unique subset of 2-aminopyrimidines based on two  $\alpha 7$ -nAChR interacting leads. Our findings based on  $\alpha 7$ -nAChR activation, subtype selectivity and binding and crystallographic structures with the AChBP show the structural basis for achieving differential interactions for nAChR selectivity within the 4,6-disubstituted 2-aminopyrimidine family.

## EXPERIMENTAL SECTION

**Materials.** (S)-(–)Nicotine, 99%, was purchased from Alfa Aesar (LO09879-14). Epibatidine (Batch no. 14A/168727), methyllycaconitine (MLA, Batch no. 20A/164724), PNU 120596 (Batch no. 2B/152009), dihydro- $\beta$ -erythroidine hydrobromide (Batch no. 9A/159234), and tropisetron hydrochloride (Batch no. 1B/152569) were purchased from Tocris. Reagents and solvents for synthesis were purchased from commercial sources in the highest purity available and used without further purification.

**Synthesis.** Reactions were performed under ambient conditions without attempts to exclude air or moisture other than capping reaction vessels. NMR spectra were obtained on Bruker Avance III 600 MHz instruments and referenced to the signals of residual 1 protium in the NMR solvent. Compounds were characterized by high-resolution mass spectrometry (HR-MS) by using an Agilent 6230 ESI-TOFMS. Analytical and preparative TLC was performed on aluminum-backed plates (EMD Chemicals, San Diego, CA) and visualized by exposure to UV light.

**Cell-Based Functional Assays.** Details are presented on the generation of stable  $Ca^{2+}$  sensing nAChR cell lines and the cell-based neurotransmitter fluorescent engineered reporters (CNiFERs).<sup>17–19</sup> Briefly, cells selected to express high levels of the specified receptor and containing the CNiFER, were cultured in 10 cm plates with DMEM (Mediatech, Manassas, VA) supplemented with 10% FBS (Gemini Bio-Products, Sacramento, CA; Atlanta Biologicals, Lawrenceville, GA) and 1% Glutamine (Invitrogen), and incubated at 37 °C with 10%  $CO_2$ . Cells were selected at 70–90% confluency and plated the day before using 100  $\mu$ L volumes per well into black, transparent flat-bottom, TC-treated 96-well plates (Thermo, Waltham, MA; E&K, Greiner Campbell, CA). On the next day, media were replaced with 100  $\mu$ L of artificial cerebral spinal fluid (aCSF). For all assays performed on  $\alpha 7$ -nAChR CNiFERs aCSF with 10  $\mu$ M of the PAM, PNU-120596 (Tocris, Ellisville, MO), was used. Plates were incubated

with buffer for 30 min at 37 °C and 10%  $CO_2$ . Agonist responses were measured in triplicate wells with the FlexStation III (SoftMax Pro 5.2, Molecular Devices) and run at 37 °C by monitoring TN-XXL FRET ratios, emissions of citrine cp174 (527 nm) to eCFP (485 nm), over 120 s with agonist injections at 30 s. A sigmoidal concentration–response (variable slope) regression of the mean peak FRET ratios was fit to generate a concentration–response curves and obtain  $EC_{50}$  values (GraphPad Prism 4).

**Protein Expression and Purification.** AChBPs were expressed and purified as previously reported.<sup>12,16</sup> Briefly, AChBP was expressed with an amino-terminal FLAG epitope tag and secreted from stably transfected HEK293S cells lacking the *N*-acetylglucosaminyltransferase I (GnTI<sup>−</sup>) gene to limit variable processing of the attached oligosaccharide termini. Protein was purified using FLAG-antibody resin, eluted with FLAG peptide (Sigma-Aldrich) and further characterized as a pentamer by size-exclusion chromatography [Superose 6 10/300GL column (GE Healthcare) in 50 mM Tris-HCl (pH 7.4), 150 mM NaCl, 0.02%  $NaN_3$ ]. The latter fractionation removed traces of contaminants and monomer. Eluants were then concentrated in a YM50 Centricon ultrafiltration unit (Millipore). Protein concentrations were determined by UV absorbance at 280 nm (NanoDrop 2000c spectrophotometer (ThermoScientific) and confirmed by the Bradford assay.<sup>16</sup>

**Radioligand Assays for Ligand Binding to AChBP.** A scintillation proximity assay (SPA)<sup>14</sup> was employed to measure ligand binding to AChBP using [<sup>3</sup>H]-epibatidine (5 nM for *Ls*-AChBP and 20 nM for *Ac*-AChBP) as the labeled ligand, polyvinyltoluene anti-mouse SPA scintillation beads (0.17 mg/mL final concentration, GE Healthcare), monoclonal anti-FLAG M2 antibody from mouse 1:8000 dilution (Sigma), and 0.50 nM AChBP in binding sites.<sup>14,16</sup> Passing initial screens for further analyses required dissociation of 50% of the bound epibatidine by 10  $\mu$ M of the candidate competitive ligand. Full concentration curves were then generated for the higher affinity ligands. Nonspecific binding was determined in parallel by adding a saturating concentration (10  $\mu$ M) of methyllycaconitine (MLA, Tocris). The resulting mixtures were allowed to equilibrate at room temperature for a minimum of 1 h and measured on a 1450 MicroBeta TriLux liquid scintillation counter (Wallac). Dissociation constants and Hill coefficients were determined from the competition profiles, using an epibatidine  $K_d$  of 0.30 nM (GraphPad Prism 4). All measurements were completed in triplicate. Nicotine dissociation of labeled epibatidine was employed as a frame of reference.

**Crystallization and Data Collection.** Complexes of multiple substituted 2-aminopyrimidines with AChBP were prepared for crystallization as described in the Supporting Information, Section 2.2. Ligand–*Ls*-AChBP complexes were formed by combining 2  $\mu$ L of a solution of a compound (10 mM dissolved in DMSO) with 48  $\mu$ L of the protein at a concentration of 5 mg/mL to achieve a stoichiometric excess of ligand to binding sites. Co-crystals were obtained by the vapor diffusion hanging drop method. Concentrated protein complex was mixed in a 1  $\mu$ L/1  $\mu$ L ratio with selected Hampton Crystal Screen Cryo solutions. Crystals approximating 0.3 mm/0.3 mm/0.2 mm dimensions were obtained using Reagent 3 (0.26 M ammonium phosphate monobasic, 35% v/v glycerol) and flash-cooled directly in liquid nitrogen. The crystallization buffer was at pH 5.

**Structure Determination.** A full set of X-ray diffraction data was collected at 100 K at the Advanced Light Source Synchrotron in Berkeley, CA (BL5.0.1). Data were processed using the HKL2000 program. Ligand–*Ls*-AChBP complex structures were solved by

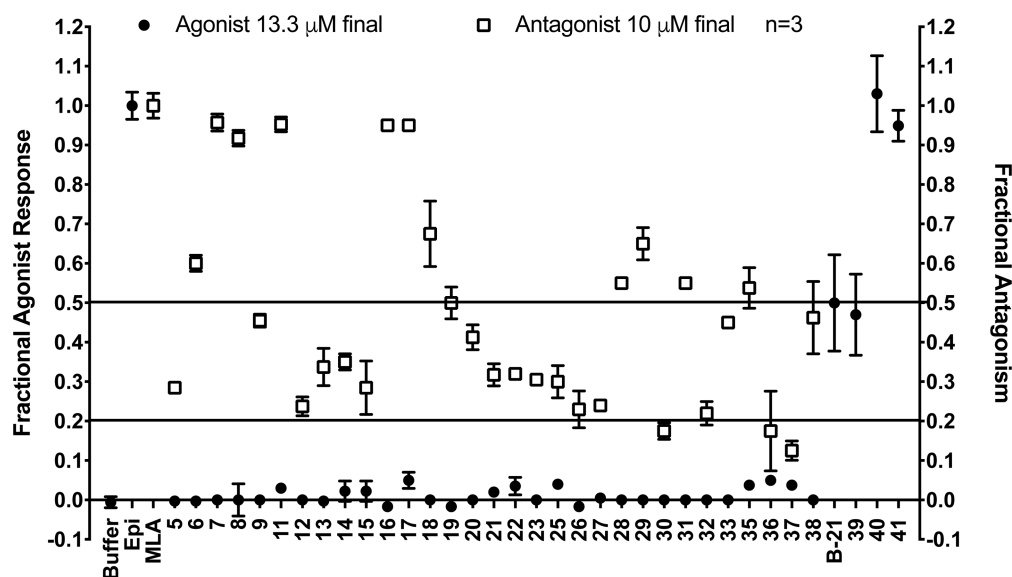


**Figure 1.** Agonist and antagonist activities of 2-aminopyrimidine series on  $\alpha 7$  nAChRs; the assays were performed with cells co-transfected with the  $\alpha 7$  nAChR and a fluorescence reporter.  $\alpha 7$ -nAChR responses were measured at 13  $\mu\text{M}$  agonist in the presence of PNU120596 (10  $\mu\text{M}$ ) compared with 100 nM epibatidine. Antagonism was determined after 30 min prior incubation with the test compounds and methyllycaconitine (MLA), prior to eliciting the 100 nM epibatidine response. Structures and AChBP binding constants for compounds 5–38 were described previously.<sup>16</sup>

molecular replacement with Phaser-MR using an ensemble of AChBP structures (PDB entry 4QAC) as the search model.

Electron density maps were fitted with COOT, Phenix-1.9-1692 was used for structure refinement. Refinement statistics are listed in Table S1 in the [Supporting Information](#). Atomic coordinates and structure parameters of the complexes have been deposited in the Protein Data Bank (PDB entries 5J5F, 5J5G, 5J5H, and 5J5I). Structural figures were generated using PyMOL.

## RESULTS

**Chemical Rationale and Synthesis.** Based on previous structure–activity considerations and X-ray crystal structures with AChBP and our lead cooperative ligands, we identified the three 2-aminopyrimidine nitrogens as key positional determinants essential for ligand–AChBP molecular recognition ([Chart 1](#)).<sup>16</sup> Consequently, we extended the study by modifying the 4,6 substituents linked to the pyrimidine ring. In directing the primary target to the  $\alpha 7$ -nAChR, only two ligands (B-21, 39) with the requisite binding affinity for AChBP met our criteria for  $\alpha 7$ -nAChR agonist activity ([Figure 1](#)). Accordingly, further syntheses were directed to the picolyl group that contained a branched chain substitution. By initially keeping an axis of symmetry at the substitutions of the amine at the 4 position, we were free to incorporate several other modifications at the 6 position in the symmetric 2-aminopyrimidine core structure. Twenty new compounds ([Table 11](#)) were generated using the synthetic [Scheme 1](#).

Commercially available 2-amino-4,6-dichloropyrimidine was reacted with appropriate secondary amines to give intermediates B-21–B-23. The amines were selected based on our initial finding showing that created branched systems as with di(2-picolyl)amine appear essential for  $\alpha 7$ -nAChR activation. In subsequent steps, intermediates in the above B series were coupled with various boronic acids using [1,1'-bis(diphenylphosphino)ferrocene] dichloropalladium(II), complex with dichloromethane or tetrakis(triphenylphosphine)-palladium(0) as a catalyst leading to products 39–55 in good to excellent yields. The electronic impact of the 6-aryl substituent was considered, therefore boronic acids were used

in syntheses encompassing different heterocycles. The aromatic rings at the 6 position were also substituted with electron-donating or electron-withdrawing substituents.

**Cell-Based Neurotransmitter Fluorescent Engineered Reporters (CNiFERs).** The synthesized series of analogues was investigated in cell-based assays, with the neurotransmitter fluorescent engineered reporter (CNiFER)<sup>17–19</sup> overexpressing  $\alpha 7$ - and  $\alpha 4\beta 2$ -nAChRs and 5-HT<sub>3A</sub> receptors (5-HT<sub>3A</sub>Rs). Concentration–response curves enabling the determination of the EC<sub>50</sub> values and Hill coefficients for the various ligands as  $\alpha 7$ -agonists are shown in [Figure 2](#). Profiles of agonist activity were all conducted in the presence of PNU120596, an  $\alpha 7$ -nAChR-positive allosteric modulator (PAM), to slow rapid formation of the desensitized state of this receptor, thereby increasing signal over the time range measured (~3 s–3 min). Activities as agonists and antagonists of the various substitutions are summarized in [Table 1](#).

**Interactions with Other Cys-Loop Receptors.** To examine selectivity for the  $\alpha 7$ -nAChR target, we also compared the activity of these ligands on the  $\alpha 4\beta 2$ -nAChR, as the most abundant of the CNS nAChRs and the 5-HT<sub>3A</sub>R as a second type of pentameric, ligand-gated cation channel. We employed epibatidine and 5-hydroxytryptamine as the respective test agonists and dihydro- $\beta$ -erythroidine and tropisetron as the respective test antagonists. Within the series of 17 compounds, only three blocked the 5-HT<sub>3A</sub>R in largely a noncompetitive manner ([Table 1](#)). Activity toward the  $\alpha 4\beta 2$ -nAChR was more complex with eight compounds showing largely noncompetitive action, but no antagonism was evident with  $K_d$ 's below 2  $\mu\text{M}$  ([Table 1](#)). The remaining compounds in the series did not exhibit detectable antagonism at concentrations of 10  $\mu\text{M}$ . Hence several compounds in the series show  $\alpha 7$ -nAChR selectivity. However, one compound 40 at submicromolar concentrations appears to enhance epibatidine activity on the  $\alpha 4\beta 2$ -nAChR. Under the conditions we used for transfection, it is likely the  $\alpha 4\beta 2$ -nAChR is assembled in two pentameric stoichiometries, ( $\alpha 4$ )<sub>3</sub>( $\beta 2$ )<sub>2</sub> and ( $\alpha 4$ )<sub>2</sub>( $\beta 2$ )<sub>3</sub>, the former forming an  $\alpha 4$ : $\alpha 4$  interface.<sup>20–22</sup> At higher concentrations

Table 1. EC<sub>50</sub> Values for  $\alpha 7$ -nAChR Agonist Activation and Antagonist Dissociation Constants for  $\alpha 4\beta 2$ -nAChR and 5HT<sub>3A</sub>R Antagonism<sup>a</sup>

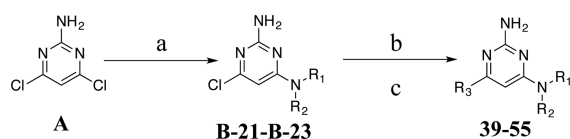
	Structure		Agonist EC <sub>50</sub> ± SD ( $\mu$ M) (n=3)	Antagonist K <sub>A</sub> ± SD ( $\mu$ M) (n=3)	
	R <sub>1</sub>	R <sub>2</sub>		$\alpha 4\beta 2$	5HT <sub>3A</sub>
39			2.5 ± 0.3*	5.7 ± 0.9 <sup>NC</sup>	>10
40			0.07 ± 0.01	6.3 ± 1.5 <sup>NC</sup> 6.3 ± 1.4 <sup>C</sup>	>10
41			0.07 ± 0.01	2.5 ± 0.8 <sup>NC</sup>	>10
42			0.14 ± 0.06	>10	>10
43			0.26 ± 0.03	>10	>10
44			0.5 ± 0.1	>10	>10
45			0.55 ± 0.10	>10	>10
46			0.6 ± 0.13	3.9 ± 0.7 <sup>C</sup> 2.9 ± 0.9 <sup>NC</sup>	15.2 ± 3.1 <sup>C</sup> 7.5 ± 1.2 <sup>NC</sup>
47			0.8 ± 0.2	>10	>10
48			1.4 ± 0.4	3.2 ± 0.5 <sup>NC</sup> 9.2 ± 1.2 <sup>C</sup>	>10
49			1.6 ± 0.2	2.4 ± 1.0 <sup>NC</sup>	>10
50			2.7 ± 0.3	>10	>10
51			3.9 ± 1.9	>10	>10
52			4.1 ± 1.3	n.t.	11.8 ± 1.4 <sup>NC</sup>
53			10.3 ± 1.4*	2.3 ± 0.8 <sup>NC</sup>	7.2 ± 0.8 <sup>NC</sup>
54			>10	>10	>10
55			>10	5.8 ± 0.7 <sup>NC</sup>	>10

<sup>a</sup>NC, non competitive; C, competitive; n.t., not tested. \* indicates partial agonist. Responses are measured from HEK cells containing a fluorescent reporter and plated as monolayers on 96-well plates.<sup>18,19</sup>

(>3  $\mu$ M), noncompetitive antagonism is evident. This will require investigation in more depth with fixed stoichiometries of these heteromeric subunit combinations forming  $\alpha 4\beta 2$ -nAChR pentamers.

**Radioligand Competition Binding Assays.** Initial characterization of the series was performed by applying a radioligand competition assay against <sup>3</sup>H-epibatidine binding at a single, 10  $\mu$ M concentration of the competing ligand. Both

epibatidine and the competing 2-aminopyrimidines were in excess of the total AChBP sites on two molluscan AChBPs from *Lymnaea stagnalis* (*Ls*-AChBP) and *Aplysia californica* (*Ac*-AChBP). Analysis of the binding constants reveals that the compounds in large part show high affinities for *Ls*-AChBP (Figure 3) and moderately high affinities for *Ac*-AChBP (Table 2). It is likely that the Tyr to Trp side chain difference at residue 55 is one, but scarcely the sole, determining factor.<sup>23</sup>

Scheme 1. Synthetic Pathway Leading to 4,6-Substituted 2-Aminopyrimidines 39–55<sup>a</sup>

<sup>a</sup>Conditions: (a) amine, DIPEA, DMF, 2–6 h; (b) boronic acid, Na<sub>2</sub>CO<sub>3</sub>, Pd(PPh<sub>3</sub>)<sub>4</sub>, toluene/ethanol, 8 h; (c) boronic acid, K<sub>2</sub>CO<sub>3</sub>, 2 M, Pd(dppf)Cl<sub>2</sub>, DMA, 8 h.

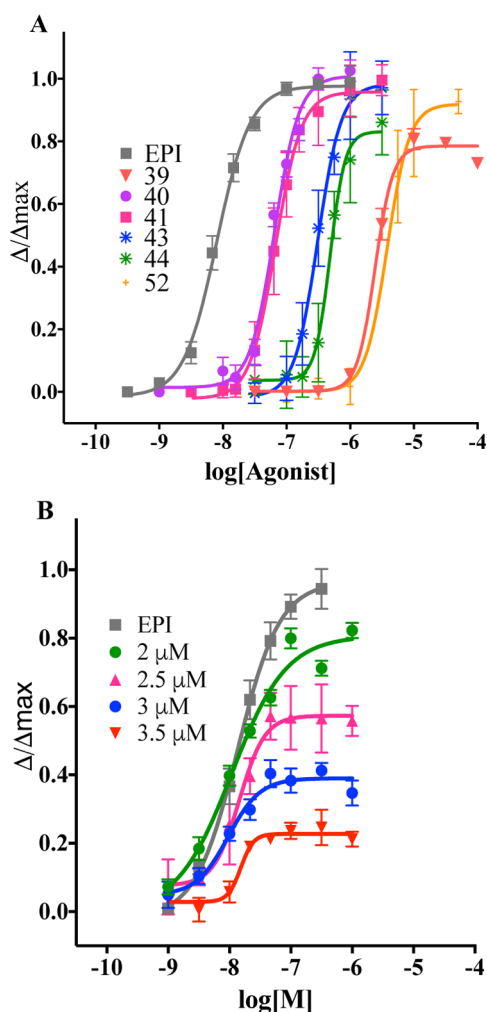


**Figure 2.** Concentration–response curves for substituted 2-aminopyrimidines on HEK-293 cells transfected with a fluorescent reporter and distinct human nAChR types: (A)  $\alpha 7$ -nAChRs in the presence of PNU 120596 and (B)  $\alpha 4/\beta 2$ -nAChRs (antagonism of epibatidine at 100 nM, compound 49). Responses are measured in 96-well plates containing a monolayer of cells with the cDNAs encoding the designated receptor and fluorescent reporter<sup>18,19</sup> with a FLIPer assay using dual emission wavelengths.

Some of the synthesized ligands showed dissociation constants as low as 20 nM, establishing that the picolyl substitution in and of itself was not compromising binding to the surrogate AChBP proteins.

**X-ray Crystallographic Analysis of the Ligands AChBP Complexes.** Representative members of the 4-picolyll and dibenzylamino 2-aminopyrimidines were co-crystallized with *Ls*-AChBP, and four X-ray data sets were collected (Figure 4):

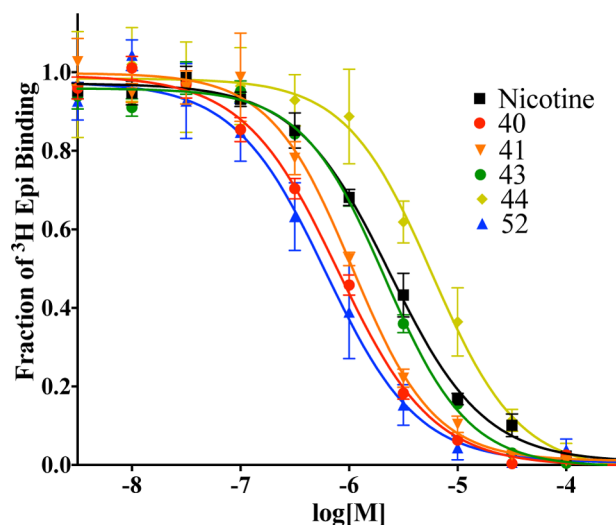


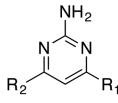
**Figure 3.** Titration of the *Ls*-AChBP–<sup>3</sup>H-epibatidine binding by the respective 4-dibenzyl- and 4-dipicolyl-substituted 2-aminopyrimidines measured using a scintillation proximity assay.<sup>14</sup>  $K_d$  values are determined from the  $K_d$  of epibatidine and the concentrations of epibatidine and competing ligand.

40 ( $K_d = 0.040 \mu\text{M}$ ), 43 ( $K_d = 0.13 \mu\text{M}$ ), 44 ( $K_d = 0.33 \mu\text{M}$ ), and 52 ( $K_d = 0.030 \mu\text{M}$ ). The structures were solved at 2.7, 2.3, 2.0, and 2.0 Å resolution, respectively, in the  $P1_{211}$  space group. The structure of *Ls*-AChBP in complex with 40 (using chains A) superimposed on 43 with an RMS deviation of 0.3 Å for 183  $\alpha$  atoms, on 44 with an RMS deviation of 0.26 Å for 186  $\alpha$  atoms, and on 52 with RMS deviation 0.26 for 176  $\alpha$  atoms. Side chain orientations show a high degree of similarity at all five binding sites in each pentamer and a similar orientation of the bound ligands. All four compounds were bound underneath of a closed C loop of the principal face at subunit junctures between the 5 subunits. Loop closure in X-ray data set of 40, as measured from the backbone carbonyl of W143 in the A loop to the  $\gamma$ -sulfur atom of the first vicinal Cys disulfide-linked residue in the C loop (C187 in *Ls*-AChBP), varies between 8.8 and 11.1 Å in ten binding sites (average of 10.3 Å). The X-ray crystal structures showed full occupancy of the protein pentamer and well-defined ligand electron densities in all binding pockets (40 is used as an example: Figure 4, panel A).

Strong polar interactions were observed for residues on the complementary face where ligand nitrogen N1, not likely protonated at physiological pH, hydrogen bonds to the Gln55 side chain (distance 2.7 Å; all distances measured for the binding pocket formed by chains C and D) and its free amino group at the position 2 hydrogen bonds to Tyr164 hydroxyl group (3.2 Å distance). In addition, the aromatic rings of the branched bis-pyridyl (picolyl) substituent may likely interact with the carbonyl of Trp143 on the principal subunit interface. Such unconventional intermolecular C=O $\cdots$  $\pi$  interactions have been studied in supramolecular frameworks, but have rarely been reported in protein crystals.<sup>24</sup> Additional stabilization could be achieved by a surrounding peptide bond framework at the binding interface.

A T-shaped  $\pi$ -stacking interaction is shown between pyridines of the dipicolyl moiety and the aromatic ring of Trp143 (3.5–3.9 Å). The nitrogens of these systems are positioned 2.7 Å away from each other, and they form dihedral angles (57 and 62°) with the carbonyl oxygen of Trp 143. Other distinctive interactions are observed with Met114 sulfur

Table 2. Dissociation Constants for 4,6-Disubstituted 2-Aminopyrimidines Determined by Competitive Back Titrations against <sup>3</sup>H-Epipatidine on SPA Beads Linked to Purified *Lymnaea stagnalis* and *Aplysia californica* AChBPs<sup>a,14</sup>

	AChBPs Binding Assay			
	<i>Ls</i> -AChBP		<i>Ac</i> -AChBP	
	$K_d \pm SD$ ( $\mu$ M)	$n_H \pm SD$	$K_d \pm SD$ ( $\mu$ M)	$n_H \pm SD$
<b>39</b>	0.16 $\pm$ 0.03	1.07 $\pm$ 0.15	0.31 $\pm$ 0.07	1.8 $\pm$ 0.4
<b>40*</b>	0.040 $\pm$ 0.003	0.91 $\pm$ 0.03	0.60 $\pm$ 0.018	1.5 $\pm$ 0.2
<b>41</b>	0.060 $\pm$ 0.005	1.16 $\pm$ 0.05	>10	-
<b>42</b>	>10	-	>10	-
<b>43*</b>	0.130 $\pm$ 0.006	1.11 $\pm$ 0.11	0.33 $\pm$ 0.05	1.25 $\pm$ 0.24
<b>44*</b>	0.33 $\pm$ 0.02	1.13 $\pm$ 0.16	>10	-
<b>45</b>	>10	-	0.083 $\pm$ 0.005	1.24 $\pm$ 0.04
<b>46</b>	0.27 $\pm$ 0.03	0.85 $\pm$ 0.01	0.062 $\pm$ 0.006	0.84 $\pm$ 0.07
<b>47</b>	>10	-	>10	-
<b>48</b>	>10	-	0.63 $\pm$ 0.09	1.12 $\pm$ 0.14
<b>49</b>	0.065 $\pm$ 0.006	1.08 $\pm$ 0.12	>10	-
<b>50</b>	0.19 $\pm$ 0.06	0.96 $\pm$ 0.02	0.07 $\pm$ 0.007	0.84 $\pm$ 0.08
<b>51</b>	>10	-	>10	-
<b>52*</b>	0.030 $\pm$ 0.001	1.00 $\pm$ 0.05	0.12 $\pm$ 0.02	1.4 $\pm$ 0.2
<b>53</b>	0.030 $\pm$ 0.004	1.09 $\pm$ 0.09	0.18 $\pm$ 0.02	0.83 $\pm$ 0.05
<b>54</b>	>10	-	>10	-
<b>55</b>	0.070 $\pm$ 0.005	1.05 $\pm$ 0.02	>10	-
<b>B-21</b>	>10	-	>10	-
<b>B-22</b>	>10	-	0.090 $\pm$ 0.004	0.80 $\pm$ 0.05
<b>B-23</b>	>10	-	>10	-

<sup>a</sup>Dissociation constants ( $K_d$ ) and Hill coefficients ( $n_H$ ) are reported as means ( $\pm$ SD). Each experiment was done in triplicate. \* indicates solved crystal structures for *Lymnaea stagnalis* AChBP ligand complexes.

atom and both sulfur atoms of the Cys187-Cys188 disulfide bridge in the C loop. These residues together align in a sandwich-type  $S/\pi$  stacking system with the pyrimidine N1 atom being 3.3 Å away from the methionine sulfur atom. The 2-methoxyphenyl ring in **40** resides on the complementary face in proximity with main hydrophobic interactions observed for Gln55, Thr56, Leu112, Tyr113, and Met114 (up to 3.2 Å for Gln55 and 3.4 Å for Thr56). The 2-methoxy substituent extends the contacts to the C loop cysteines with the methoxy oxygen located 3.5 Å from both sulfur atoms.

When the X-ray crystal structure of **40** was aligned with the *Ls*-AChBP:nicotine complex (PDB code: 1UW6), striking differences in ligand positioning along with some differences in protein side chain orientations were observed (Figure 4, panel D). Both pyridyl rings of **40** occupy the nicotine site where ring nitrogens overlap with those of nicotine. Most significant side chain differences are observed on the principal subunit for Tyr89, Tyr185, Cys 187–188, and for Gln55, Leu112, Met114 and Tyr164 on the complementary face.

Major dissimilarities were also apparent when the X-ray crystal structure of **40** was compared to crystal structures of cooperative ligands (Figure 4, panels E and F). Here again only the pyridyl rings of **40** exhibited some superimposition with the cooperative ligands. In the complex with **15** (Figure 4, panel E), the greatest differences are seen for Tyr185, Cys 187–188 (principal subunit), and Gln55 on the complementary subunit. In case of the structure of negatively cooperative ligand, **33** (Figure 4, panel F), side chain differences are much more evident, especially for Tyr185, Cys 187–188 (principal

subunit), and Trp53, Gln55, Met114, and Tyr164 (complementary subunits).

The cation-binding selectivity of nAChRs<sup>1–4,23</sup> is distinctive. Quaternary amines are stabilized by cation- $\pi$  interactions with a nest of surrounding aromatic side chains, whereas other interactions with protonated secondary and tertiary amines and imines are often stabilized by hydrogen bonding to the backbone carbonyl of W143.<sup>13,25</sup> Typically the quaternary amine or a strongly basic tertiary amine or imine is accompanied another ring system or region of the molecule that can serve as a hydrogen bond acceptor, the pyridine in nicotine, epibatidine or anabaseine or the keto group in cytosine or anatoxin. Hence, a common chemotype is also evident for the less basic nitrogen and candidate other H-bond acceptors.

The 2-aminopyrimidines appear to diverge from this pattern as distinctly different orientations of this core ring are evident in the bound structures (compare Figure 4, panels D–F) and the three nitrogens of the 2-aminopyrimidine motif are only weakly basic. Thus, a cationic form of the 2-aminopyrimidine is not likely to be the bound species as found for the more strongly basic pyrrole, aza-bicyclic, and imine ring systems.

Moreover, the orientation of the 2-aminopyrimidine ring differs in the structures of compounds that bind only to AChBP vs those that bind to both AChBP and activate the  $\alpha 7$ -nAChR (Figure 4, panels E and F). We suggest that the bulky, branched nature of the dibenzylamine or picolylamine substituents drives this change, leading to an important difference in eliciting  $\alpha 7$  agonist activity. The necessity for adopting two distinct orientations for the 2-aminopyrimidine ring perhaps explains

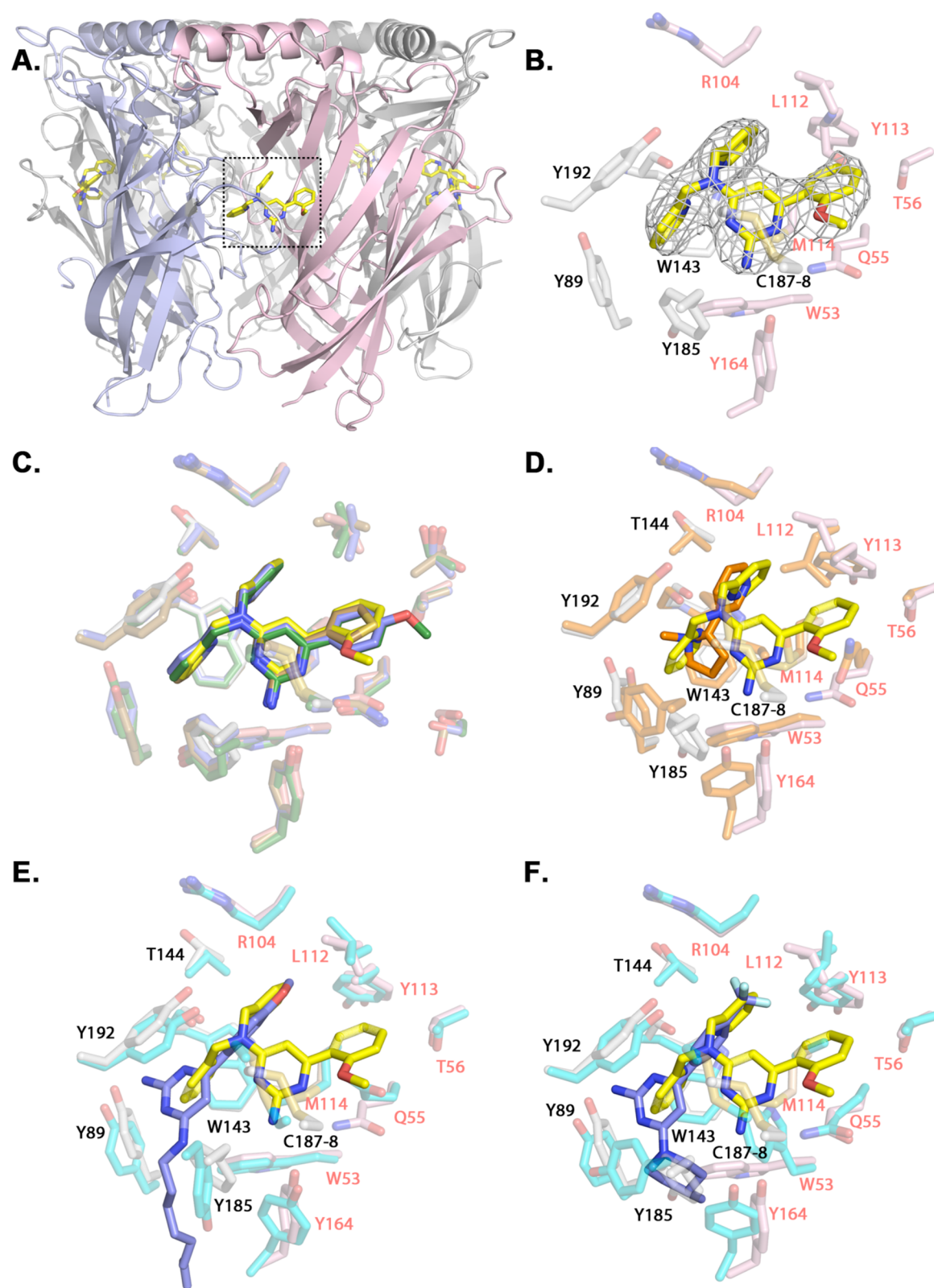


**Figure 4.** X-ray crystal structures of ligands 40, 43, 44, and 52 in complex with *Ls*-AChBP and their comparison with 1UW6, 4QAA and 4QAC. (A) Radial view of *Ls*-AChBP pentameric structure in complex with 40. A principal, C loop-containing, and complementary face are shown in violet and fuchsia. (B) Expanded radial view of 40 in the binding site. Side chain carbons of the principal (gray) and complementary (fuchsia) subunits are designated with black and red numbers, respectively. Ligand carbons displayed in yellow, nitrogens in blue, oxygen in red. (C) Superimposition of X-ray crystal structure of 40, that interacts more extensively with Gln55 and the Cys-loop S–S bridge in the *Ls*-AChBP with X-ray crystal structures of 43, 44, and 52. (D) Superimposition of 40 with nicotine (PDB code 1UW6, in orange). (E) Superimposition of 40 with positively cooperative ligand 15 (PDB code 4QAA; ligand carbons shown in blue, protein in turquoise). (F) Superimposition of 40 with negatively cooperative ligand 33 (PDB code 4QAC).

why only 2 of nearly 40 initial compounds elicited  $\alpha 7$ -nAChR responses.

## DISCUSSION

Presynaptic, homomeric  $\alpha 7$ -nAChRs are present on glutaminergic and other terminals whose activation facilitates neurotransmitter release in several brain regions, including the hippocampus, cortex and ventral tegmental area.<sup>1–5</sup> Hence  $\alpha 7$ -nAChRs are believed play important roles in modulating neurotransmission, cognition, sensory gating and anxiety. Accordingly, great interest is generated in  $\alpha 7$ -nAChR modulation that targets cognitive symptoms particularly in disorders of development, such as schizophrenia, and in dementias associated with aging, such as Parkinson's and Alzheimer's diseases.

Several new and redesigned nAChR agonists with the capacity to cross the blood–brain barrier have shown cognitive improvements in animal testing.<sup>26–32</sup> These compounds are typically amines, such as nicotine and epibatidine, or imines, such as anabaseines. They contain a moderately strong base and interact as a protonated form to associate with a backbone carbonyl oxygen on the principal subunit interface and also possess a dipole or weaker base that interacts with positions on the complementary subunit at the subunit interface. Among the compounds, several are in phase II or III or earlier stages of development and testing.<sup>29–32</sup> Failure rates due to adverse side effects and limited efficacy are high, suggesting a need for new structural landscapes that can either activate  $\alpha 7$ -AChRs more selectively or produce enhanced therapeutic indices through other CNS receptors.

Our approach to structure-guided drug design in this study employs a soluble surrogate of the nAChR to obtain leads of unique structure with an assay of through-put comparable to synthetic generation of newly designed agents. With candidate leads, more laborious cell-based screens of functional responses and crystallographic studies enable one to determine binding poses. Molecular or atomic-based determinants on the ligand and target conferring higher affinity and selectivity can then be assigned. Since both the  $\alpha 7$ -nAChR and AChBP are homomeric, they become a logical starting point for reiterative structure–activity studies involving the extracellular domain of the receptor. We have found this ligand design sequence to be more productive, since attempts to convert AChBP to become more  $\alpha 7$ -nAChR-like in sequence and selectivity have been limited by instability of the successive mutant gene products.<sup>23</sup>

Interestingly, AChBP binding was gained by altering the 2-aminopyrimidine structure with branched substituents. Although positive cooperativity of ligand binding and responses was evident with nicotine on the  $\alpha 7$ - and other nAChRs, Hill coefficients hovering around 1.0 were found for nicotine binding with *Ls*-AChBP. By contrast, several of the 2-aminopyrimidines exhibited cooperative values. However, of the group of ~40 compounds, only two showed appreciable affinity for the  $\alpha 7$ -nAChR. Using these leads, we were able to find substituents preferred by the  $\alpha 7$ -nAChR. Since only a minority of compounds were interacting with both homomeric pentamers, the AChBPs may offer more than a single binding mode for the 2-aminopyrimidine family of ligands.

Although we see a substantial departure in selectivity between the marine and fresh water mollusks, with some compounds we find comparable affinities that cross into being an effective  $\alpha 7$ -nAChR agonist. Compound **39** interacted with both *Lymnaea* and *Aplysia* AChBPs ( $K_d = 0.16 \mu\text{M}$ ,  $n_H = 1$  and

( $K_d = 0.31 \mu\text{M}$ ,  $n_H = 1.8$ ) as well as activated  $\alpha 7$ -nAChRs at 2.5  $\mu\text{M}$  (Tables 2 and 1, **39**). The combination of modest cooperativity in *Ac*-AChBP binding with activation of  $\alpha 7$ -nAChR convinced us to select it as our new lead for the second reiteration of structure and generation of nAChR active compounds. Hence, high-resolution structure-guided ligand design through a receptor surrogate appears to provide novel landscapes for  $\alpha 7$ -agonist leads.

## ASSOCIATED CONTENT

### Supporting Information

The Supporting Information is available free of charge on the ACS Publications website at DOI: 10.1021/jacs.6b10746.

Chemical synthesis and characterization; NMR, HR-MS, and crystallographic information (PDF)

## AUTHOR INFORMATION

### Corresponding Author

\*pwtaylor@ucsd.edu

### ORCID

M. G. Finn: 0000-0001-8247-3108

Palmer Taylor: 0000-0002-3081-131X

### Present Address

<sup>§</sup>M.H.: Department of Structural Biology, Weizmann Institute of Science, Rehovot 76100, Israel

### Author Contributions

<sup>‡</sup>K.K. and G.A.C.H. contributed equally to this work.

### Notes

The authors declare no competing financial interest.

## ACKNOWLEDGMENTS

The work was supported by the National Institutes of Health Grant GM 18360-44 (to P.T.), the Tobacco-related Disease Research Program 21FT\_0024 (to K.K.), and a Graduate Training Fellowship from CONACYT (Mexico, to G.A.C.H.). We thank the UCSD Chemistry and Biochemistry Molecular MS facility and Brendan M. Duggan from the UCSD School of Pharmacy for providing high-field NMR assistance. Kwok-Yiu Ho, Limin Zhang, Dr. Zoran Radic, and members of the beamline staff and The Advanced Light Source, Lawrence Berkeley National Laboratory provided expertise, engaging discussions and valued suggestions.

## REFERENCES

- Changeux, J. P. *J. Biol. Chem.* **2012**, *287*, 40207.
- Dineley, K. T.; Pandya, A. A.; Yakel, J. L. *Trends Pharmacol. Sci.* **2015**, *36*, 96.
- Thompson, A. J.; Lester, H. A.; Lummis, S. C. Q. *Rev. Biophys.* **2010**, *43*, 449.
- Bertrand, D.; Lee, C.-H.; Flood, D.; Marger, F.; Donnelly-Roberts, D. *Pharmacol. Rev.* **2015**, *67*, 1025.
- Taly, A.; Corringer, P. J.; Guedin, D.; Lestage, P.; Changeux, J. P. *Nat. Rev. Drug Discovery* **2009**, *8*, 733.
- Stokes, C.; Treinin, R.; Papke, R. L. *Trends Pharmacol. Sci.* **2015**, *36*, 514.
- Gill-Thind, J. K.; Dhankher, P.; D'Oyley, J. M.; Sheppard, T. D.; Millar, N. S. *J. Biol. Chem.* **2015**, *290*, 3552.
- Smit, A. B.; Syed, N. I.; Schaap, D.; van Minnen, J.; Klumperman, J.; Kits, K. S.; Lodder, H.; van der Schors, R. C.; van Elk, R.; Sorgedraeger, B.; Brejc, K.; Sixma, T. K.; Geraerts, W. P. *Nature* **2001**, *411*, 261.
- Brejc, K.; van Dijk, W. J.; Klaassen, R. V.; Schuurmans, M.; van Der Oost, J.; Smit, A. B.; Sixma, T. K. *Nature* **2001**, *411*, 269.



- (10) Hansen, S. B.; Radic, Z.; Talley, T. T.; Molles, B. E.; Deerinck, T.; Tsigelny, I.; Taylor, P. *J. Biol. Chem.* **2002**, *277*, 41299.
- (11) Rucktooa, P.; Smit, A. B.; Sixma, T. K. *Biochem. Pharmacol.* **2009**, *78*, 777.
- (12) Hansen, S. B.; Talley, T. T.; Radic, Z.; Taylor, P. *J. Biol. Chem.* **2004**, *279*, 24197.
- (13) Hibbs, R. E.; Sulzenbacher, G.; Shi, J.; Talley, T. T.; Conrod, S.; Kem, W. R.; Taylor, P.; Marchot, P.; Bourne, Y. *EMBO J.* **2009**, *28*, 3040.
- (14) Talley, T. T.; Yalda, S.; Ho, K.-Y.; Tor, Y.; Soti, F. S.; Kem, W. R.; Taylor, P. *Biochemistry* **2006**, *45*, 8894.
- (15) Shi, J.; Koeppe, J. R.; Komives, E. A.; Taylor, P. *J. Biol. Chem.* **2006**, *281*, 12170.
- (16) Kaczanowska, K.; Radic, Z.; Changeux, J. P.; Finn, M. G.; Taylor, P. *Proc. Natl. Acad. Sci. U. S. A.* **2014**, *111*, 10749.
- (17) Nguyen, Q. T.; Schroeder, L. F.; Mank, M.; Muller, A.; Taylor, P.; Griesbeck, O.; Kleinfeld, D. *Nat. Neurosci.* **2010**, *13*, 127.
- (18) Yamauchi, J. G.; Nemezc, A.; Nguyen, T. Q.; Muller, A.; Schroeder, L. F.; Talley, T. T.; Lindstrom, J.; Kleinfeld, D.; Taylor, P. *PLoS One* **2011**, *6*, e16519.
- (19) Yamauchi, J. G.; Gomez, K.; Grimster, N. P.; Dufouil, N.; Nemezc, A.; Fotsing, J. R.; Ho, K.-Y.; Talley, T. T.; Sharpless, K. B.; Fokin, V. V.; Taylor, P. *Mol. Pharmacol.* **2012**, *82*, 687.
- (20) Da Silva-Tavares, X.; Blum, A. P.; Nakamura, D. T.; Puskar, N. L.; Shanata, J. A. P.; Lester, H. A.; Dougherty, D. A. *J. Am. Chem. Soc.* **2012**, *134*, 11474.
- (21) Eaton, J. B.; Lucero, L. M.; Stratton, H.; Chang, Y.; Cooper, J. F.; Lindstrom, J. M.; Lukas, R. J.; Whiteaker, P. *J. Pharmacol. Exp. Ther.* **2014**, *348*, 46.
- (22) Mazzaferro, S.; Gasparri, F.; New, K.; Alcaino, C.; Faundez, M.; Iturriaga-Vasquez, P.; Vijayan, R.; Biggin, P. C.; Bermudez, I. *J. Biol. Chem.* **2014**, *289*, 21795.
- (23) Nemezc, A.; Taylor, P. *J. Biol. Chem.* **2011**, *286*, 42555.
- (24) Wan, C.-Q.; Chen, X.-D.; Mak, T. C. W. *CrystEngComm* **2008**, *10*, 475.
- (25) Grimster, N. P.; Stump, B.; Fotsing, J. R.; Weide, T.; Talley, T. T.; Yamauchi, J. G.; Nemezc, A.; Kim, C.; Ho, K.-Y.; Sharpless, K. B.; Taylor, P.; Fokin, V. V. *J. Am. Chem. Soc.* **2012**, *134*, 6732.
- (26) Arunrungvichian, K.; Fokin, V. V.; Vajragupta, O.; Taylor, P. *ACS Chem. Neurosci.* **2015**, *6*, 1317.
- (27) Arunrungvichian, K.; Boonyarat, C.; Fokin, V. V.; Taylor, P.; Vajragupta, O. *ACS Chem. Neurosci.* **2015**, *6*, 1331.
- (28) Jaikhan, P.; Boonyarat, C.; Arunrungvichian, K.; Taylor, P.; Vajragupta, O. *Chem. Biol. Drug Des.* **2016**, *87*, 39.
- (29) Horenstein, N. A.; Papke, R. L.; Kulkarni, A. R.; Chaturbhuj, G. U.; Stokes, C.; Manther, K.; Thakur, G. A. *J. Biol. Chem.* **2016**, *291*, 5049.
- (30) Vukelic, M.; Qing, X.; Redecha, P.; Koo, G.; Salmon, J. E. *J. Immunol.* **2013**, *191*, 1800.
- (31) Gault, L. M.; Ritchie, C. W.; Robieson, W. Z.; Pritchett, Y.; Othman, A. A.; Lenz, R. A. *Alzheimers Dement.* **2015**, *1*, 81.
- (32) Umbricht, D.; Keefe, R. S.; Murray, S.; Lowe, D. A.; Porter, R.; Garibaldi, G.; Santarelli, L. *Neuropsychopharmacology* **2014**, *39*, 1568.